LA-UR- 08-4978

Approved for public release; distribution is unlimited.

Title:	in situ PEM Fuel Cell Water Measurements
Author(s):	Rod L. Borup Mukundan Rangachary John R Davey Jacob Spendelow Tommy Rockward Muhammad Arif David Jacobson
Submitted to:	2008 Fuel Cell Seminar

in situ PEM Fuel Cell Water Measurements

Rodney L. Borup, Rangachary Mukundan, John R Davey, Jacob Spendelow, Tommy Rockward,
Los Alamos National Laboratory; MPA-11, MS J579, P.O. Box 1663, Los Alamos, NM 87545
Muhammad Arif, David Jacobson, Daniel Hussey, National Institute of Standards and Technology; 100 Bureau Dr., Mail Stop 8461, Gaithersburg, Maryland 20899-8461

Efficient PEM fuel cell performance requires effective water management. The materials used, their durability, and the operating conditions under which fuel cells run, make efficient water management within a practical fuel cell system a primary challenge in developing commercially viable systems. We present experimental measurements of water content within operating fuel cells, in response to operational conditions, including transients and freezing conditions.

To help understand the effect of components and operations, we examine water transport in operating fuel cells, measure the fuel cell water *in situ* and model the water transport within the fuel cell. High Frequency Resistance (HFR), AC Impedance and Neutron imaging (using NIST's facilities) were used to measure water content in operating fuel cells with various conditions, including current density, relative humidity, inlet flows, flow orientation and variable GDL properties. Ice formation in freezing cells was also monitored both during operation and shut-down conditions.

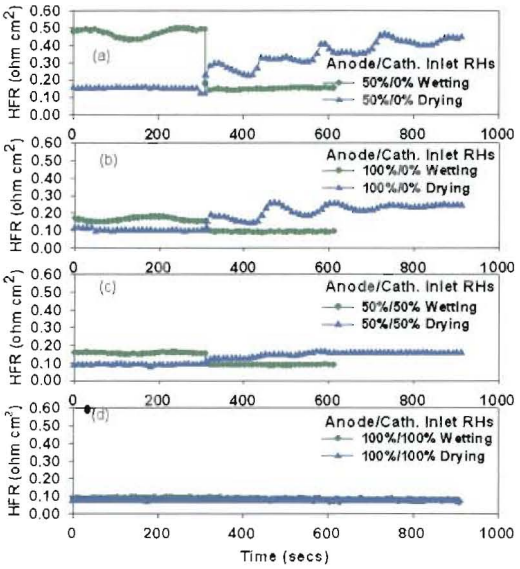

Figure 1. Increasing current "wetting" and decreasing current "drying" step transients at 300 seconds at 80°C and various inlet relative humidities. (a) 50%/0%, (b) 100%/0%, (c) 50%/50% and (d) 100%/100% anode/cathode RH.

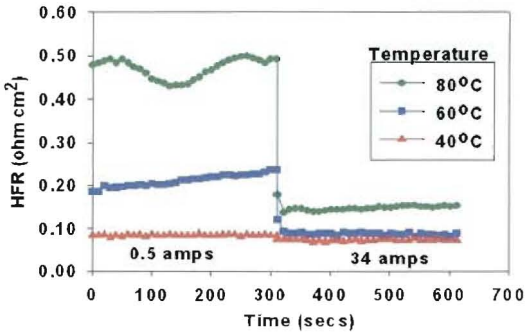

Figure 2. Wetting responses at 40°C, 60°C, and 80°C for anode and cathode gas inlet RHs of 50% and 0%.

Water Response to Operating Transients

Automotive polymer electrolyte membrane (PEM) fuel cells will likely operate with inlet gas streams at less than saturated conditions and will experience numerous and varied power transients. Both of these factors will affect the water dynamics of the MEA as well as other fuel cell components. The response of cell water was measured to power transients by applying step changes to the cell current with varied RHs. "Wetting" transients (current step from 0.5 to 34 amp) show a faster HFR drop (10-30 seconds) than the HFR increase (several minutes) seen in the reciprocal "drying" transients (34 to 0.5 amp) (see Figure 1). This is true for operating temperatures of 40, 60 and

80°C and all examined combinations of anode and cathode gas inlet RHs. This suggests that reaction water created at the cathode electrode quickly back-diffuses through the membrane, accounting for the fast wetting of the MEA. This back-diffusion wetting-time scale is similar to the 10 seconds identified by Wang[1,2]. The drier the inlet gas RHs, the greater the observed HFR change in both the current transient wetting and drying responses (Figure 1). This is primarily due to the higher HFR levels reached at these dry gas inlet conditions, which translated to lower MEA water content. The current wetting response rate, at the same gas inlet RHs of 50% anode / 0% cathode, for 40°C, 60°C, and 80°C are similar; in the range of 10 – 30 seconds. However, the drying response to the 34 to 0.5 amp current transient is faster at higher operating temperatures (Figure 2). This faster drying response at higher temperature is most likely due to the greater drying effect of the warmer cathode air. The water holding capacity of 80°C air, at the same RH, is more than 6 times greater than that at 40°C.

Neutron Imaging Profiles

Neutron radiography was used to measure water distribution profiles *in situ* within an operating PEMFC to develop a greater understanding of the water concentration and location within the fuel cell. High resolution water imaging of fuel cells using a Micro-Channel Plate (MCP) detector [3] with 25 μm resolution produces water profile images in which one can distinguish between water in anode and cathode gas diffusion layers (GDLs), as well as between water in the GDLs above channels and above lands, and water in the channels themselves.

Water generated at the MEA during fuel cell operation must be transported through either the anode or cathode GDLs to be removed via the flow fields. For water generated under a land, it must first be transported to the GDL that is under a channel in order to escape into the flow field. Therefore, the amount of water in parts of the MEA, as well as in the GDLs that are under lands, is generally higher than the amount of water under channels. A typical image is illustrated in Fig. 3.

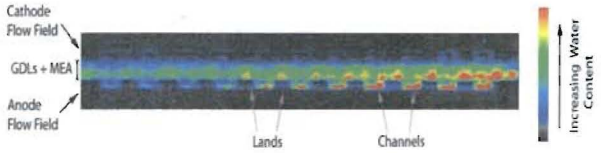

Figure 3. Water density image from high resolution neutron radiography.

Using neutron imaging, the amount of water in particular parts of the cell can be quantitatively calculated. Figure 4a shows the amount of water in the fuel cell MEA (catalyst layers and membrane) during a cell operated with gas co-flow, and with gas counter-flow. Figure 4b shows the water for the same conditions including the water in the anode, cathode and GDLs. During co-flow operation, water produced in the MEA must be removed by transport through the GDLs to the flow fields. The amount of water (vapor and/or liquid) in the flow fields must increase down the length of the cell (from inlet to outlet) as the generated water is removed through the flow fields. As the amount of

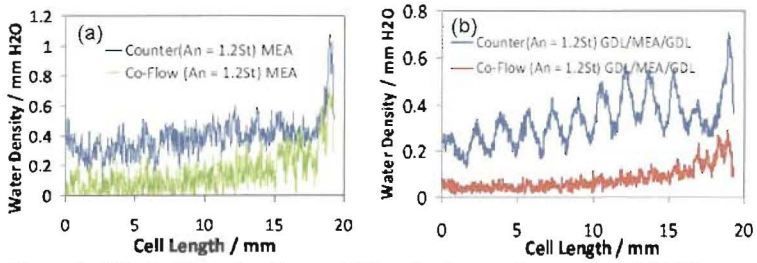

Figure 4. Effect of flow direction on MEA water for a cell operating at 80 °C, anode stoichiometry = 1.2, cathode stoichiometry = 2, 100% RH anode feed, 0% RH cathode feed, current density = 1.5 A cm^{-2}. (a) MEA, (b) GDLs and MEA.

water vapor and/or liquid in the flow fields increases down the length of the cell, a higher concentration of water in the MEA is needed to continue to drive the flux of generated water out of the MEA, through the GDLs and into the flow fields. Therefore, MEA water content increases monotonically from inlet to outlet. The situation is different when a counter-flow configuration is employed. Starting at the anode inlet (left side of Figure 4), the water content in the anode flow field is low, while the water content across the GDLs in the cathode flow field is significantly higher (since the cathode stream has picked up generated water, which is exiting the cell through the cathode outlet) . Therefore, a net flux of water occurs from the cathode flow field toward the anode flow field. At the same time, a portion of the generated water produced in this part of the cell is driven into the anode flow field. Therefore, the water content in the anode flow field initially increases moving from the anode inlet toward the anode outlet. Since the amount of water in the anode flow field increases when moving in this direction, the amount of water in the cathode flow field also increases, since less of the water on the cathode side has diffused across to the anode side at this point in the cell. Both flow fields have a higher water content moving from the left towards the middle of the cell, and as a result the MEA also has a higher water content. The situation changes moving closer to the right side of the cell. Since this side is closer to the cathode inlet, the cathode stream has not yet picked up as much water as it eventually will, and the lower water content on the cathode side results in a driving force for transport of water from the anode side to the cathode side. This lowers the amount of water in the anode flow field, and since both flow fields have lower water content towards the right side of the cell, the MEA water is also consequently lower.

In summary, both anode and cathode streams accumulate generated water as they flow through the cell, and they remove some of this generated water as they exit the cell. However, near the inlets/outlets, there is also a significant driving force for transport of water from the outlet portion of each flow field across the GDLs and the MEA to the inlet portion of the opposing flow field. Therefore, the amount of water in the middle portion of the cell tends to be higher than it is in the vicinity of the inlets/outlets.

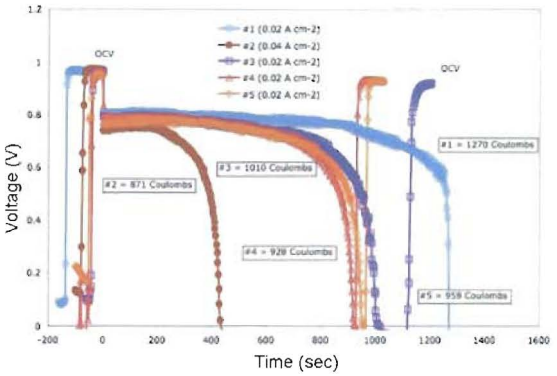

Figure 5. The performance of fuel cell operated in 500 cc min^{-1} of dry H_2 and air at constant temperature of -10 °C using a Gore™ Primea® MEA

Operation at sub-freezing temperatures:

The performance of a single cell operated at -10 °C, with a Gore™ MEA is illustrated in Figure 5. The cell voltage drops as expected, due to ice formation at the cathode inhibiting further electrochemical reaction. The constant current operations (Figure 5.) illustrate the wide variability in the amount of charge (871 to 1270 Coulombs) that can be passed before the voltage decays to zero. This charge represents the water/ice carrying capacity of the cell at sub-freezing temperatures and as previously

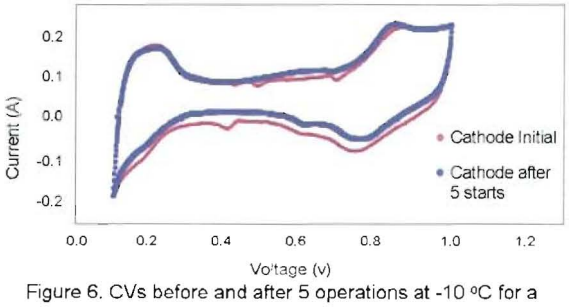

Figure 6. CVs before and after 5 operations at -10 °C for a LANL MEA

illustrated is a function of initial membrane water content (λ) and current density.[4] However, unlike the measurements at -20 °C,[4] these results actually indicate a decrease in the amount of charge that can be passed as the cell water content is decreased. For example, in start #1 the initial voltage at a current density of 0.02 A cm^{-2} is 0.81 V and the charge capacity is 1270 Coulombs. However, in start #5, the initial voltage is 0.764 V and the charge capacity is only 958 Coulombs. These results indicate that the nature of ice formation at -10 °C and - 20°C may be different.

To distinguish between changes in the MEA versus changes in the GDL, cyclic voltammograms obtained after each successive operation at -10 °C were analyzed. This is illustrated in Figure 6 where cathode CVs for a LANL MEA before the first cold start operation and after the 5th cold start operation are compared. There is very little change in the electrochemical catalyst surface area (ECSA) after 5 cold start operations at -10 °C. However, the CVs performed on the Gore™ MEA exhibit a significant loss (> 50% loss) in the ECSA at the cathode (see Figure 7). On the other hand there is no loss in the ECSA at the anode of that same cell. These results indicate that the cathode catalyst layer on the Gore™ MEAs is affected significantly more than the catalyst layer on the LANL MEA. This helps reconcile some of the differences observed in the literature where Ge et al.[5] reported a loss in ECSA whereas Mukundan et al.[6] reported no loss in ECSA after cold start operations at -10 °C and -20 °C. This illustrates the importance of the catalyst layer morphology to the durability of PEM fuel cells operated at sub-freezing temperatures. One possible explanation could be the fact that the water may not freeze in a catalyst layer with very small pore sizes, while it will freeze in a catalyst layer with larger pores (not enough depression in the freezing point). Ishikawa et al. reported that the water in the catalyst layer of their MEA did not freeze at -10 °C and was present as a super-cooled liquid state that only froze on the surface after warming to 0 °C[7]. Neutron imaging of this water/ice was performed to confirm this hypothesis.

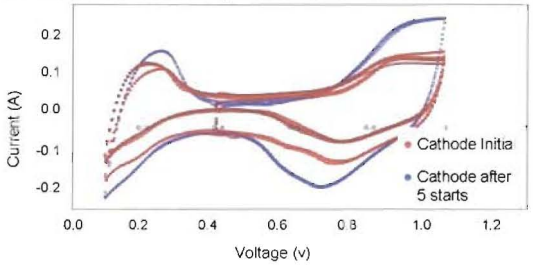

Figure 7. CVs before and after 5 operations at -10 °C for the Gore™ MEAs

*GORE, and PRIMEA are trademarks of W. L. Gore & Associates, Inc.

References

1. Yun Wang and C. Y. Wang, *Electrochimica Acta 50 (2005) 1307-1315*
2. Yun Wang and C. Y. Wang, *Electrochimica Acta 51 (2006) 3924-3933*
3. D .S. Hussey, D. L. Jacobson, K .J. Coakley, D. F. Vecchia, and M. Arif, *2007 Proceedings of the ASME 5th International Conference on Fuel Cell Science, Engineering and Technology*, New York, NY (2007).
4. E. L. Thompson, J. Horne, W. Gu, H. A. Gasteiger, *J. Electrochem. Soc.*, **155(6)**, B625 (2008).
5. S. Ge, C. Y. Wang, *J. Electrochem. Soc.*, **154(12)**, B1399 (2007).
6. R. Mukundan, Y. S. Kim, T. Rockward, J. R. Davey, B. Pivovar, D. Hussey, D. Jacobson, M. Arif, R. Borup, *ECS Transaction*, **11(1)**, 411 (2007).
7. Y. Ishikawa, T. Morita, K. Nakata, K. Yoshida, and M. Shiozawa, *J. Power Sources*, **163**, 708 (2007).